

Entanglement generation resonances in XY chains

R. Rossignoli, C.T. Schmiegelow

Departamento de Física-IFLP, Universidad Nacional de La Plata,

C.C.67, La Plata (1900), Argentina

Abstract

We examine the maximum entanglement reached by an initially fully aligned state evolving in an XY Heisenberg spin chain placed in a uniform transverse magnetic field. Both the global entanglement between one qubit and the rest of the chain and the pairwise entanglement between adjacent qubits is analyzed. It is shown that in both cases the maximum is not a monotonous decreasing function of the aligning field, exhibiting instead a resonant behavior for low anisotropies, with pronounced peaks (a total of $[n/2]$ peaks in the global entanglement for an n -spin chain), whose width is proportional to the anisotropy and whose height remains finite in the limit of small anisotropy. It is also seen that the maximum pairwise entanglement is not a smooth function of the field even in small finite chains, where it may exhibit narrow peaks above strict plateaus. Explicit analytical results for small chains, as well as general exact results for finite n -spin chains obtained through the Jordan-Wigner mapping, are discussed.

PACS numbers: 03.67.Mn, 03.65.Ud, 75.10.Jm

I. INTRODUCTION

Quantum entanglement has been long recognized as one of the most fundamental and intriguing features of quantum mechanics [1]. It denotes the ability of composite quantum systems to develop correlations which have no classical counterpart. Interest on all aspects of entanglement has grown enormously since its potential for permitting radically new forms of information transmission and processing was unveiled [2, 3, 4, 5], being now considered an essential *resource* in the field of quantum information science [6], where rigorous entanglement measures have been introduced [7, 8]. The interest has also extended to other areas like condensed matter physics, where it has provided a novel perspective for the analysis of correlations and quantum phase transitions [9, 10, 11, 12, 13].

Spin systems with Heisenberg interactions [14, 15] constitute a particularly attractive scenario for studying quantum entanglement. They provide a scalable qubit representation suitable for quantum processing tasks [16, 17, 18, 19] and can be realized by diverse physical systems such as cold atoms in optical lattices [20], quantum dots [16, 17] and Josephson junctions arrays [21]. Accordingly, several investigations of entanglement in ground and thermal equilibrium states of Heisenberg spin chains subject to an external magnetic field have been made (see for instance [9, 10, 11, 12, 22, 23, 24]). There have also been relevant studies of entanglement dynamics in spin chains (for instance [18, 25, 26, 27, 28, 29]), which discuss in particular the evolution of initial Bell states and the ensuing “entanglement waves” [25], non-ergodicity and dynamical phase transitions starting with equilibrium states [26], decoherence waves [27], evolution in varying magnetic fields [28], generation of cluster states [29] as well as other issues.

In the present work we want to focus on a particular aspect, namely the generation of entanglement in an interacting spin chain with fixed parameters starting from an initially fully separable aligned state, and examine the maximum entanglement that can be reached as a function of the anisotropy and the uniform transverse magnetic field (control parameter). We will concentrate here on the *global* entanglement between one qubit and the rest of the chain and on the *pairwise* entanglement between neighboring qubits, within the context of a cyclic XY chain with nearest neighbor interactions [14]. Questions which immediately arise include the possible existence of a threshold anisotropy for reaching maximum global entanglement (saturation), the maximum pairwise entanglement that can be reached and,

most important, the behavior with the applied magnetic field. It will be shown that contrary to what can be naively expected, the maximum global entanglement reached is not a monotonous function of the aligning field, but exhibits instead a typical *resonant behavior* for low anisotropies, with narrow peaks located at characteristic field values, entailing a high sensitivity suitable for entanglement control. The pairwise entanglement exhibits a more complex resonant response, since it is affected by a competition between two incompatible types (essentially of positive or negative spin parity). These resonances *remain finite* in the limit of vanishing (but non-zero) anisotropy in finite chains, considering sufficiently long time evolutions. On the other hand, for large anisotropies they merge into a single broad maximum centered at zero field, with global saturation reached within a field window.

Our results are based on a fully exact treatment of the finite n -spin chain based on the Jordan-Wigner transformation [14], explicitly verified for the case of two and three-qubit chains. The Hamiltonian and the entanglement measures employed are discussed in section II. Section III contains the results, discussing first the two and three-qubit cases and then the exact results for general n -qubit chains. Finally, conclusions are drawn in IV.

II. FORMALISM

We consider n qubits or spins in a cyclic chain interacting through an XY nearest neighbor coupling, embedded in a uniform transverse magnetic field [14, 15]. The Hamiltonian reads

$$H = bS^z - \sum_{j=1}^n (v_x s_j^x s_{j+1}^x + v_y s_j^y s_{j+1}^y) \quad (1a)$$

$$= bS^z - \frac{1}{2} \sum_{j=1}^n (v s_j^+ s_{j+1}^- + g s_j^+ s_{j+1}^+ + h.c.), \quad (1b)$$

where $S^z = \sum_{j=1}^n s_j^z$ is the total spin along the direction of the magnetic field b , $v, g = (v_x \pm v_y)/2$ and $n+1 \equiv 1$. We will consider the evolution of the state which is initially fully aligned antiparallel to the magnetic field,

$$|\Psi(t)\rangle = \exp[-iHt] |\downarrow \dots \downarrow\rangle, \quad (2)$$

where t denotes time over \hbar , and examine the emerging *global* entanglement between one qubit and the rest of the chain, as well as the *pairwise* entanglement between contiguous

qubits, arising for non-zero anisotropy $\gamma = g/v$ (for $g = 0$ the initial state is an eigenstate of H and hence no entanglement is generated).

Since we are dealing with a pure state, the first one is determined by the entropy [7]

$$E_1 = -\text{Tr} \rho_1 \log_2 \rho_1, \quad (3)$$

of the reduced *one-qubit* density $\rho_1 = \text{Tr}_{n-1} \rho$, where $\rho = |\Psi(t)\rangle\langle\Psi(t)|$ is the full density matrix, with $E_1 = 0$ for ρ_1 pure ($\rho_1^2 = \rho_1$) and $E_1 = 1$ (maximum) for ρ_1 fully mixed. The second one is the entanglement of formation [7] of the adjacent *pair* density $\rho_2 = \text{Tr}_{n-2} \rho$, which can be calculated as [8]

$$E_2 = -\sum_{\nu=\pm} q_\nu \log_2 q_\nu, \quad (4)$$

where $q_\pm = (1 \pm \sqrt{1 - C_2^2})/2$ and

$$C_2 = \text{Max}[2\lambda_m - \text{Tr} R, 0], \quad R = \sqrt{\rho_2 \tilde{\rho}_2}, \quad (5)$$

is the *concurrence* [8], with λ_m the greatest eigenvalue of R and $\tilde{\rho}_2 = 4s_j^y s_{j+1}^y \rho_2^* s_{j+1}^y s_j^y$ the spin-flipped density. It satisfies $0 \leq C_2 \leq 1$. Since tracing out qubits of a subsystem can be considered a LOCC (local operations and classical communication) transformation, it cannot increase entanglement [7] and hence $E_2 \leq E_1$, with $E_2 = E_1$ for a pure two qubit state (in which case q_\pm become the eigenvalues of ρ_1).

As E_2 is just an increasing function of C_2 , pairwise entanglement is usually directly measured through the latter, which is more suitable for analytic description. The corresponding measure of the global E_1 entanglement is the square root of the *one-tangle* [8],

$$C_1 = 2\sqrt{\text{Det} \rho_1} = \sqrt{2(1 - \text{Tr} \rho^2)}, \quad (6)$$

which coincides with C_2 for a pure two qubit state and satisfies $C_1 \geq C_2$ in the general case (actually the more general inequality $C_i \geq \sqrt{\sum_{j \neq i} C_{ij}^2}$, with C_{ij} the concurrence of the (i, j) pair and C_i^2 the one-tangle of qubit i , conjectured in [30], was recently proven [31]). Both E_1 and C_1 are measures of the disorder associated with ρ_1 and are hence increasing functions of one another.

Due to the symmetries of H and the present initial state, $|\Psi(t)\rangle$ will be invariant under translation ($j \rightarrow j + 1$) and inversion ($j \rightarrow n + 1 - j$), and will have *positive spin parity* $P = \exp[i\pi(S^z + n/2)]$, as this quantity is preserved by H ($[H, P] = 0$). The reduced

density $\rho_S = \text{Tr}_{n-S}\rho$ of *any* subsystem S will then depend just on the distance between its components and will *commute* with the subsystem parity $P_S = \prod_{j \in S} \exp[i\pi(s_j^z + 1/2)]$, as the reduction involves just diagonal elements in the rest of the chain. In the case of ρ_1 , this implies that it will be the same for all qubits and *diagonal* in the standard basis $|\uparrow\rangle, |\downarrow\rangle$ of s^z eigenstates:

$$\rho_1 = \begin{pmatrix} p(t) & 0 \\ 0 & 1 - p(t) \end{pmatrix}, \quad (7)$$

where $p(t)$ represents the one-qubit spin flip probability

$$p(t) = \langle s_j^z \rangle_t + 1/2 = \langle S^z \rangle_t / n + 1/2, \quad (8)$$

(here $\langle O \rangle_t \equiv \langle \Psi(t) | O | \Psi(t) \rangle$ and spin operators are considered dimensionless). Hence,

$$C_1(t) = 2\sqrt{p(t)[1 - p(t)]}, \quad (9)$$

with $C_1(t) = 1$ when $p(t) = 1/2$.

The same symmetries lead to a pair density of the form

$$\rho_2 = \begin{pmatrix} p_1(t) & 0 & 0 & \alpha^*(t) \\ 0 & p_2(t) & \beta(t) & 0 \\ 0 & \beta(t) & p_2(t) & 0 \\ \alpha(t) & 0 & 0 & p_3(t) \end{pmatrix}, \quad (10)$$

in the standard basis $|\uparrow\uparrow\rangle, |\uparrow\downarrow\rangle, |\downarrow\uparrow\rangle, |\downarrow\downarrow\rangle$, where $p_1(t) + 2p_2(t) + p_3(t) = 1$, $p_1(t) + p_2(t) = p(t)$ and

$$\alpha(t) = \langle s_j^+ s_{j+1}^+ \rangle_t, \quad \beta(t) = \langle s_j^+ s_{j+1}^- \rangle_t, \quad (11a)$$

$$p_1(t) = \langle (s_j^z + 1/2)(s_{j+1}^z + 1/2) \rangle_t, \quad (11b)$$

for adjacent qubits. Eq. (5) becomes then

$$C_2(t) = 2 \text{Max} [|\alpha(t)| - p_2(t), |\beta(t)| - \sqrt{p_1(t)p_3(t)}, 0], \quad (12)$$

where only one of the entries can be positive (this follows from the positivity of ρ_2 , which requires $|\alpha(t)| \leq \sqrt{p_1(t)p_3(t)}$, $|\beta(t)| \leq p_2(t)$). Two kinds of pairwise entanglement can therefore arise: type I ($|\alpha(t)| > p_2(t)$) and type II ($|\beta(t)| > \sqrt{p_1(t)p_3(t)}$), which cannot coexist and can then be present just at *different* times, and which stem from the positive (I) and negative (II) parity sectors of ρ_2 .

The eigenvalues of H and the entanglement of its eigenstates are obviously independent of the sign of g , and for even chains also of the sign of v , as for n even it can be changed by a transformation $s_j^{x,y} \rightarrow (-1)^j s_j^{x,y}$. Due to time reversal symmetry, the emerging entanglement in even chains will then be also independent of the sign of b , while in odd chains that for $(-b, v)$ will coincide with that for $(b, -v)$. We will then set in what follows $v \geq 0$, $g \geq 0$, and consider both signs of b .

III. RESULTS

A. Two qubit case

Let us first analyze this simple situation, which nonetheless provides already some insight on the behavior for general n . Here $C_1 = C_2 \forall t$. The evolution subspace is spanned by the states $|\downarrow\downarrow\rangle, |\uparrow\uparrow\rangle$, and the pertinent eigenstates of H are $|\pm\rangle = u_{\mp}|\downarrow\downarrow\rangle \mp u_{\pm}|\uparrow\uparrow\rangle$, with energies $E_{\pm} = \pm\lambda$, where $u_{\pm} = \sqrt{(\lambda \pm b)/(2\lambda)}$ and $\lambda = \sqrt{b^2 + g^2}$. The state (2) will then be independent of v and given by

$$\begin{aligned} |\Psi(t)\rangle &= \sum_{\nu=\pm} e^{-iE_{\nu}t} \langle \nu | \downarrow\downarrow \rangle | \nu \rangle \\ &= (\cos \lambda t + i \frac{b}{\lambda} \sin \lambda t) |\downarrow\downarrow\rangle + i \frac{g}{\lambda} \sin \lambda t |\uparrow\uparrow\rangle, \end{aligned} \quad (13)$$

so that the spin-flip probability $p(t)$ is

$$p(t) = \frac{g^2}{b^2 + g^2} \sin^2 \lambda t. \quad (14)$$

Its maximum $p_m = g^2/(b^2 + g^2)$ is thus a *Lorentzian of width g* centered at $b = 0$, satisfying $p_m \geq 1/2$ if $|b| \leq g$. Hence, for *any* $g > 0$ the system will always reach *maximum entanglement* $C_1 = 1$ within the field window $|b| \leq g$, at times t_m such that $p(t_m) = 1/2$, where Eq. (13) becomes a type I Bell state:

$$|\Psi(t_m)\rangle = \pm i (|\uparrow\uparrow\rangle + e^{\pm i\phi} |\downarrow\downarrow\rangle) / \sqrt{2}, \quad \cos \phi = b/g.$$

The maximum concurrence reached (Fig. 1) is then

$$C_1^m = C_2^m = \begin{cases} 1, & |s| \leq 1 \\ \frac{2|s|}{s^2+1}, & |s| \geq 1 \end{cases}, \quad s = b/g, \quad (15)$$

which is *higher* than the concurrence $C^\pm = g/\lambda$ of the Hamiltonian eigenstates $\forall b \neq 0$, becoming $\approx 2g/|b|$ for $|b| \gg g$. $C_1(t)$ will follow the evolution of $p(t)$ if $p_m \leq 1/2$ ($|s| \leq 1$), but will develop saturated maxima plus an intermediate minima when $p_m > 1/2$.

We also note that for $b = 0$, i.e., where the gap $E_+ - E_- = 2\lambda$ is minimum and vanishes for $g \rightarrow 0$, maximum entanglement can in principle be attained for *any* $g > 0$. In this case the eigenstates $|\pm\rangle$ become *independent* of g and maximally entangled, and none of them approaches the aligned initial state for $g \rightarrow 0$ (in contrast with the behavior for $b \neq 0$). The initial state becomes then equally distributed over both eigenstates ($u_\pm = 1/\sqrt{2}$) $\forall g > 0$, implying $|\Psi(t)\rangle = \cos gt|\downarrow\downarrow\rangle + i \sin gt|\uparrow\uparrow\rangle$. Hence, in this case the only limit for reaching maximum entanglement ($\sin^2 gt = 1/2$) for arbitrarily small but non-zero g is the long waiting time ($t_m = \pi/(4g)$). We will see that an analogous situation will occur for any n at particular field values.

B. Three qubit case

For $n = 3$, the evolution subspace is still two-dimensional and spanned by $|\downarrow\downarrow\downarrow\rangle$ and the W -state [32] $|W\rangle \equiv (|\downarrow\uparrow\uparrow\rangle + |\uparrow\downarrow\uparrow\rangle + |\uparrow\uparrow\downarrow\rangle)/\sqrt{3}$, which for $g = 0$ have energies $-3b/2$ and $b/2 - v$. The coupling induced by g leads to eigenstates $|\pm\rangle = u_\mp|\downarrow\downarrow\downarrow\rangle \mp u_\pm|W\rangle$ with energies $E_\pm = \varepsilon \pm \lambda$, where $u_\pm = \sqrt{[\lambda \pm (b - v/2)]/(2\lambda)}$, $\varepsilon = -(b + v)/2$ and $\lambda = \sqrt{(b - v/2)^2 + 3g^2/4}$. We then obtain

$$|\Psi(t)\rangle = e^{-i\varepsilon t}[(\cos \lambda t + i\frac{b-v/2}{\lambda} \sin \lambda t)|\downarrow\downarrow\downarrow\rangle + i\frac{\sqrt{3}g}{2\lambda} \sin \lambda t|W\rangle]$$

which leads to

$$p(t) = \frac{g^2}{2[(b - v/2)^2 + 3g^2/4]} \sin^2 \lambda t. \quad (16)$$

Its maximum $p_m = g^2/(2\lambda^2)$ is again a Lorentzian of width proportional to g but centered at $b = v/2$ due to the hopping term, where $p_m = 2/3$ (the value at the W -state), with $p_m \geq 1/2$ for $|b - v/2| \geq g/2$. Hence, for *any* $g \neq 0$ there is again a field interval where *maximum* E_1 entanglement is attained. The maximum of $C_1(t)$ (Fig. 1, top right) is then

$$C_1^m = \begin{cases} 1, & |s| \leq 1/2 \\ \frac{\sqrt{2s^2+1/2}}{s^2+3/4}, & |s| \geq 1/2 \end{cases}, \quad s = (b - v/2)/g. \quad (17)$$

For $|b| \gg v, g$, $C_1^m \approx \sqrt{2}g/|b|$, an asymptotic result which turns out to be *valid* $\forall n \geq 3$. The evolution of $C_1(t)$ remains qualitatively similar to that for $n = 2$. Note also that for

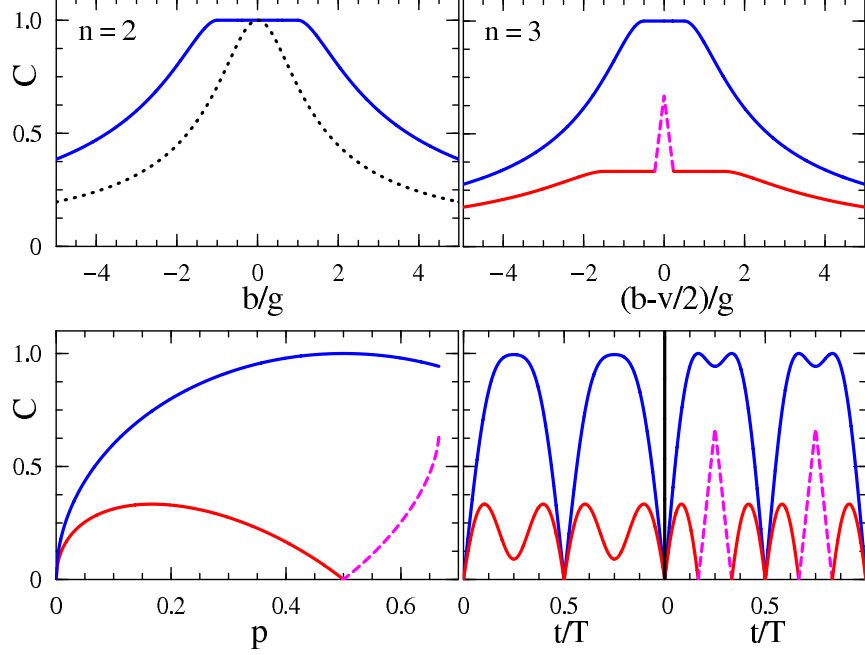


FIG. 1: (Color online). Top: Left: Maximum entanglement (measured by the concurrence) reached by the two qubit chain as a function of the (scaled) magnetic field for an initially aligned state. The dotted line depicts the concurrence of the Hamiltonian eigenstates. Right: Maximum global concurrence C_1^m between one-qubit and the rest (upper curve, in blue) and maximum pairwise concurrence C_2^m (lower curve, in red+dashed pink) in the three qubit system, in terms of the (shifted+scaled) magnetic field. C_2^m exhibits a sharp type II resonance at $b = v/2$. Bottom: Left: Plot of C_1 and C_2 in the three qubit chain in terms of the spin flip probability p ($0 \leq p \leq 2/3$). Right: The temporal evolution of C_1 and C_2 in the three qubit chain at the C_2^m plateau ($b = v/2 \pm 0.6g$, left) and at resonance ($b = v/2$, right). $T = 2\pi/\lambda$ is the period. Type I (II) sectors in C_2 are depicted in solid red (dashed pink) lines.

$b = v/2$, i.e., where the gap 2λ is minimum and vanishes for $g = 0$, maximum C_1 is again reached for any $g > 0$, the situation being similar to that for $n = 2$ at $b = 0$.

The behavior of the pairwise entanglement is, however, more complex. The W -state contains type II pairwise entanglement, but $|\Psi(t)\rangle$ will first develop that of type I, so that transitions between both types can be expected to occur in the evolution for large g . From the expression of $|\Psi(t)\rangle$ we obtain $|\alpha(t)| = \sqrt{p(t)(2-3p(t))}/2$, $p_2(t) = p_1(t) = \beta(t) = p(t)/2$, so that Eq. (12) becomes

$$C_2(t) = |\sqrt{p(t)[2-3p(t)]} - p(t)|, \quad (18)$$

which corresponds to type I (II) for $p(t) < 1/2$ ($> 1/2$). It is thus a non-monotonous function of $p \equiv p(t)$ (left bottom panel in Fig. 1), having a maximum at $p = 1/6$ (where $C_2 = 1/3$), vanishing at the “critical” value $p = 1/2$ (where C_1 is maximum) and increasing again for $p > 1/2$ up to its absolute maximum at the endpoint $p = 2/3$, where $C_2 = 2/3$ (i.e., the value at the W -state). Hence, saturation ($C_2 = 1$) cannot be reached. Moreover, it is verified that $C_2(t)/C_1(t) \leq 1/\sqrt{2}$ (the maximum ratio allowed by the generalized inequality [30] for $C_{12} = C_{13}$), the maximum reached for $p \rightarrow 0$ or $p \rightarrow 2/3$. The evolution of $C_2(t)$ will then not follow that of $p(t)$ or $C_1(t)$ if $p_m > 1/6$, developing for $p_m < 1/2$ a minimum when $p(t)$ is maximum, which will evolve into two vanishing points plus a type II maximum if $p_m > 1/2$ (see right bottom panel in Fig. 1). The maximum of $C_2(t)$ is then

$$C_2^m = \begin{cases} \frac{1/2-|s|}{s^2+3/4}, & |s| \leq s_c \\ 1/3, & s_c \leq |s| \leq 3/2 \\ \frac{|s|-1/2}{s^2+3/4}, & |s| \geq 3/2 \end{cases}, \quad s = \frac{b-v/2}{g} \quad (19)$$

where $s_c = \sqrt{3} - 3/2 \approx 0.23$ determines the second point where $C_2 = 1/3$ and encloses the region of dominant type II entanglement. It then exhibits *a sharp type II peak at $b = v/2$* , above a strict *type I plateau* (see Fig. 2). Note that at $b = v/2$, $C_2^m = 2/3$ for *any* $g > 0$, as in this case the system will always reach the W -state if the waiting time is sufficiently long ($t_m = \pi/(\sqrt{3}g)$). For $|b| \gg v, g$, $C_2^m \approx g/|b| \approx C_1^m/\sqrt{2}$, an asymptotic result *which is again valid* $\forall n \geq 3$.

C. General n

By means of the Jordan-Wigner transformation [14], we may exactly convert the Hamiltonian (1) within a fixed spin parity subspace ($P = \pm 1$) to a quadratic form in fermion operators c_j^\dagger, c_j , defined by $c_j^\dagger = s_j^+ \exp[-i\pi \sum_{l=1}^{j-1} s_l^+ s_l^-]$. For a finite cyclic chain with positive parity $P = 1$, the result for $H' = H + bn/2$ is

$$H' = \sum_{j=1}^n bc_j^\dagger c_j - (\frac{1}{2} - \delta_{jn})(vc_j^\dagger c_{j+1} + gc_j^\dagger c_{j+1}^\dagger + h.c.) \quad (20a)$$

$$= \sum_k (b - v \cos \omega_k) c_k^\dagger c_k' - \frac{1}{2}g \sin \omega_k (c_k^\dagger c_{-k}^\dagger + c_{-k}' c_k'), \quad (20b)$$

where the fermion operators $c'_k, c'_k{}^\dagger$ are related to c_j, c_j^\dagger by a finite Fourier transform

$$c_j^\dagger = \frac{e^{i\pi/4}}{\sqrt{n}} \sum_k e^{i\omega_k j} c'_k{}^\dagger, \quad \omega_k = 2\pi k/n,$$

with k *half-integer* for the present cyclic conditions: $k = -\frac{n-1}{2}, \dots, \frac{n-1}{2}$ for n even and $k = -\frac{n}{2} + 1, \dots, \frac{n}{2}$ for n odd. We then obtain the diagonal form

$$\begin{aligned} H' &= \sum_k \lambda_k a'_k{}^\dagger a_k - \frac{1}{2} [\lambda_k - (b - v \cos \omega_k)], \\ \lambda_k &= \sqrt{(b - v \cos \omega_k)^2 + g^2 \sin^2 \omega_k}, \end{aligned} \quad (21)$$

by a means of a BCS-like transformation $c'_k{}^\dagger = u_k a'_k{}^\dagger + v_k a_{-k}$, $c'_{-k} = u_k a_{-k} - v_k a'_k{}^\dagger$ to quasi-particle fermion operators $a'_k{}^\dagger, a_k$, with $u_k^2, v_k^2 = [\lambda_k \pm (b - v \cos \omega_k)] / (2\lambda_k)$. The quasiparticle energies (21) are two-fold degenerate ($\lambda_k = \lambda_{-k}$) except for $k = n/2$ for n odd.

We can now determine the exact evolution for any n . In the Heisenberg representation ($dO/dt = i[H, O]$), we have $a'_k{}^\dagger(t) = e^{i\lambda_k t} a'_k{}^\dagger(0)$, $a_k(t) = e^{-i\lambda_k t} a_k(0)$, and the ensuing contractions

$$\langle a'_k{}^\dagger(t) a_k(t) \rangle_0 = v_k^2, \quad \langle a'_k{}^\dagger(t) a'_{-k}(t) \rangle_0 = -u_k v_k e^{2i\lambda_k t},$$

with respect to the present initial state (vacuum of the operators c, c'). The average of any operator can now be evaluated by substitution and use of Wick's theorem [33].

1. Evaluation of $p(t)$ and $C_1(t)$

The one-qubit spin flip probability becomes

$$p(t) = \langle c_j^\dagger(t) c_j(t) \rangle_0 = \frac{2}{n} \sum'_k \frac{g^2 \sin^2 \omega_k}{\lambda_k^2} \sin^2 \lambda_k t, \quad (22)$$

where $\sum'_k \equiv \sum_{k=1/2}^{[n/2]-1/2}$ ($[n/2]$ denotes integer part). For $n = 2, 3$ the sum in (22) reduces to a single term ($k = 1/2$, with $\omega_k = \pi/2$ and $\pi/3$ respectively) and we recover *exactly* Eqs. (14) and (16).

For $n \geq 4$, the evolution of $p(t)$ will be in general quasiperiodic. Its upper envelope can nevertheless be obtained setting $\sin^2 \lambda_k t = 1 \forall k$ in (22):

$$p(t) \leq p_m = \frac{2}{n} \sum'_k \frac{g^2 \sin^2 \omega_k}{(b - v \cos \omega_k)^2 + g^2 \sin^2 \omega_k}, \quad (23)$$

the maximum of $p(t)$ lying arbitrarily close to p_m for sufficiently long time intervals (except for rational ratios $\lambda_k/\lambda_{k'}$). For low $g \ll v$, p_m will then exhibit $[n/2]$ peaks, located at

$$b = b_k \equiv v \cos \omega_k, \quad k = \frac{1}{2}, \dots, [\frac{n}{2}] - \frac{1}{2}, \quad (24)$$

(i.e. $\omega_k = \pi/n, 3\pi/n, \dots, (2[n/2] - 1)\pi/n$), which are the fields where the quasiparticle energies $\lambda_{\pm k}$ are minimum and vanish for $g \rightarrow 0$. Hence, they are located symmetrically around $b = 0$ for even n ($b_{[n/2]-k} = -b_k$), with a peak at $b = 0$ ($k = n/4$) for $n/2$ odd, but asymmetrically for odd n . Moreover, while for $b \neq b_k$, $p_m \propto g^2$, vanishing for $g \rightarrow 0$, at $b = b_k$ p_m remains finite $\forall g \neq 0$, with $p_m \rightarrow 2/n$ for $g \rightarrow 0$ (Eq. 23). This implies

$$C_1^m \rightarrow 2\sqrt{\frac{2}{n}(1 - \frac{2}{n})}, \quad (25)$$

at $b = b_k$ for $g \rightarrow 0$ and $n \geq 4$ (and $C_1^m \rightarrow 1$ for $n = 2, 3, 4$ as in these cases $2/n \geq 1/2$). Thus, by adjusting the field it is always possible to achieve, in principle, *finite* E_1 entanglement even for arbitrarily low (but non-zero) values of g . The effect of low anisotropies is just to determine the *width* of these peaks, given by $\approx g|\sin \omega_k|$ in p_m , which increases as g increases or as $|b_k|$ decreases.

The evolution at $b = b_k$ becomes purely harmonic for $g \rightarrow 0$, with

$$p(t) \rightarrow \frac{2}{n} \sin^2 \lambda_k t, \quad \lambda_k = g \sin \omega_k. \quad (26)$$

The maximum of $p(t)$ is first reached at $t_k = \pi/(2g \sin \omega_k)$, so that the smaller the value of g (or ω_k), the longer it will take to reach the maximum. In this sense, while the maximum entanglement reached in an unbounded time interval is not a continuous function of g for $g \rightarrow 0$ at $b = b_k$, that reached in a *finite* interval $[0, t_f]$ will actually vanish for $g \rightarrow 0$ also at $b = b_k$, in agreement with the result for $g = 0$, becoming lower than (25) if $t_f < t_k$.

The situation at the resonances $b = b_k$ is thus similar to that encountered for $n = 2$ at $b = 0$ or for $n = 3$ at $b = v/2$. At $b = b_k$ the energy gap $2\lambda_k$ between positive parity states with the pair $(k, -k)$ occupied and empty (in particular that between the quasiparticle vacuum $|0_q\rangle$ and the state $a_k^\dagger a_{-k}^\dagger |0_q\rangle$) is minimum, *vanishing* for $g \rightarrow 0$ (level crossings). Due to these degeneracies, at $b = b_k$ the aligned state is not approached by any of the Hamiltonian eigenstates for $g \rightarrow 0$, remaining distributed over essentially two eigenstates. The previous limits (25)-(26) can then be directly derived from Eq. (20b), where for $g \rightarrow 0$ and $b = b_k$, we may conserve just the $\pm k$ terms in the g -interaction. The evolution subspace in this limit

is then spanned by the original fermionic vacuum $|0\rangle$ (the present initial state) and the two particle state $|k, -k\rangle = c_k^\dagger c_{-k}^\dagger |0\rangle$, with g -independent eigenstates $|\pm\rangle = (|0\rangle \mp |k, -k\rangle)/\sqrt{2}$ of perturbed energies $\pm g \sin \omega_k$ (i.e., $\pm \lambda_k$). We then obtain (omitting a global phase)

$$|\Psi(t)\rangle \rightarrow \cos \lambda_k t |0\rangle + i \sin \lambda_k t |k, -k\rangle, \quad (27)$$

for the fermionic $|\Psi(t)\rangle$, which leads immediately to Eq. (26). The factor $2/n$ is just the average occupation $\langle c_j^\dagger c_j \rangle = \sum_{k'} \langle c_{k'}^\dagger c_{k'} \rangle / n$ in the state $|k, -k\rangle$.

As g increases, the resolutions of the individual peaks diminish, merging eventually into a single broad peak centered at $b \approx 0$. Since the separation between maxima is $\delta b \approx (2\pi v/n)|\sin \omega_k|$, we have the approximate bound $g \lesssim \pi v/n$ for visible individual peaks. On the other hand, it is to be noticed that for $n \geq 5$ maximum E_1 entanglement can be reached only above a certain *threshold* value g_c of g (and then within a certain field window), with $g_c \leq v \forall n$ since at $b = 0$ and $g = v$ we have exactly $p_m = (2/n) \sum_k' \sin^2 \omega_k = 1/2$ for *any* n . In fact, $g_c \approx v$ for large n . For $g \gg (v, b)$, $p_m \rightarrow 1$ ($1 - 1/n$) for n even (odd), so that saturation in C_1 is always reached. Finally, for large fields $|b| \gg v, g$,

$$p_m \approx \frac{2g^2}{nb^2} \sum_k' \sin^2 \omega_k = \frac{g^2}{2b^2}, \quad n \geq 3, \quad (28)$$

implying $C_1^m \approx \sqrt{2}g/|b|$. This asymptotic result is *independent* of n (for $n \geq 3$) and coincident with the result previously obtained for $n = 3$.

Results for $n = 4, 5$ and $14, 15$ are shown in Figs. 2 and 3. For $n = 4$, the resonances are located at $b_k = \pm v/\sqrt{2}$, with $p_m \geq 1/2$ (and hence $C_1^m = 1$) for $|b^2 - v^2/2| \leq g^2/2$. This determines two saturated plateaus in C_1^m centered at $b = b_k$ for $g < v$, which merge into a *single* plateau centered at $b = 0$ for $g > v$. For $n = 5$ the peaks are located at $b_k = v(1 \pm \sqrt{5})/4 \approx 0.81, -0.31$, where $C_1^m \rightarrow 2\sqrt{6}/5 \approx 0.98$ for $g \rightarrow 0$ (Eq. 25). Saturation is reached only for $g/v \gtrsim 0.67$, initially just at the right peak, although for $g > v$, C_1^m exhibits again a saturated plateau covering $b = 0$. For $n = 14$ (15), $C_1^m \rightarrow 0.7$ (0.68) at the seven peaks for $g \rightarrow 0$, and saturation is reached for $g \gtrsim 0.92$.

The small or tiny dips in the numerical result for C_1^m that can be seen in Figs. 2 and 3 arise due to the occurrence of rational ratios between the quasiparticle energies λ_k at particular values of b/v , in which case the maximum of $p(t)$ can be lower than the smooth upper envelope (23). For instance, for $n = 4$ the ratio of the two distinct energies $\lambda_{1/2}, \lambda_{3/2}$ becomes 2 at $|b|/v = \sqrt{2}(5 \pm \sqrt{16 - 9\gamma^2})/6$ (provided $\gamma < 4/3$), where the maximum

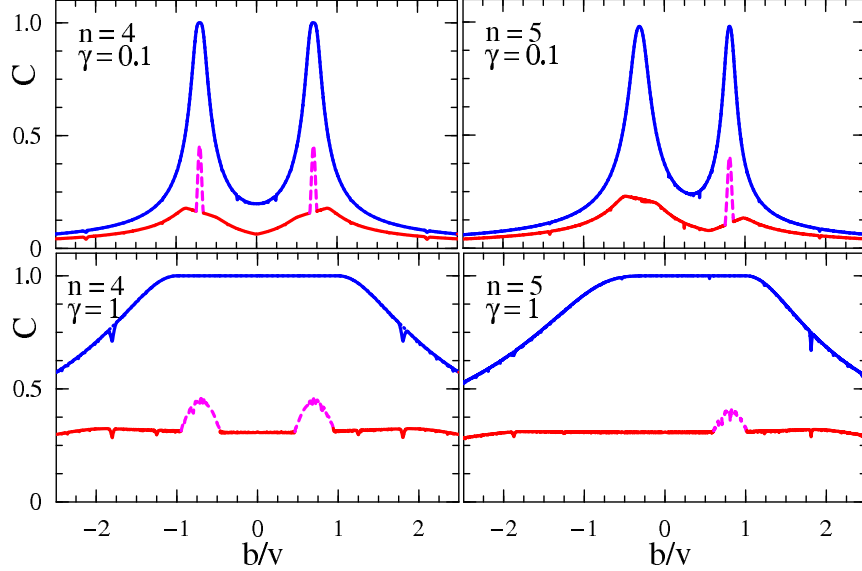


FIG. 2: (Color online). Maximum concurrence between one qubit and the rest (upper blue curves) and between adjacent qubits (lower red+dashed pink curves), reached in the four (left) and five (right) qubit chains for two different anisotropies $\gamma = g/v$ (type II sectors in C_2 depicted again with dashed pink lines). For $n = 4$ the peaks in the global concurrence at $b/v = \pm 1/\sqrt{2}$ are no longer resolved for $\gamma \geq 1$, but remain in the pairwise concurrence. For $n = 5$, the resonances are located at $b/v = (1 \pm \sqrt{5})/4$ and merge again in a saturated maximum for $\gamma \geq 1$, while the pairwise concurrence presents a type II resonance just at the second peak, which again remains visible for large γ . Dotted lines in the upper curves depict results obtained with the upper envelope (23), and are almost coincident with the numerically obtained maximum in the interval $0 \leq vt \leq 40$. See text for more details.

reached by $p(t)$ is just $(4/5)p_m$ (20% reduction). A reduction in the maximum of $p(t)$ will also occur in the vicinity of these values of $|b|/v$ for finite time intervals. This effect gives rise to the noticeable dip in C_1^m at $|b|/v \approx 1.8$ for $\gamma = 1$ (the other value $|b|/v \approx 0.55$ lies within the plateau region and its effect on C_1^m is unobservable) and to those at $|b|/v \approx 0.24$ and ≈ 2.12 for $\gamma = 0.1$.

It should be also mentioned that for short times $\lambda_k t \ll 1 \forall k$, $p(t)$ becomes independent of n , its series expansion of order m remaining stable for $n > m$. For instance, up to $O((\lambda_k t)^4)$

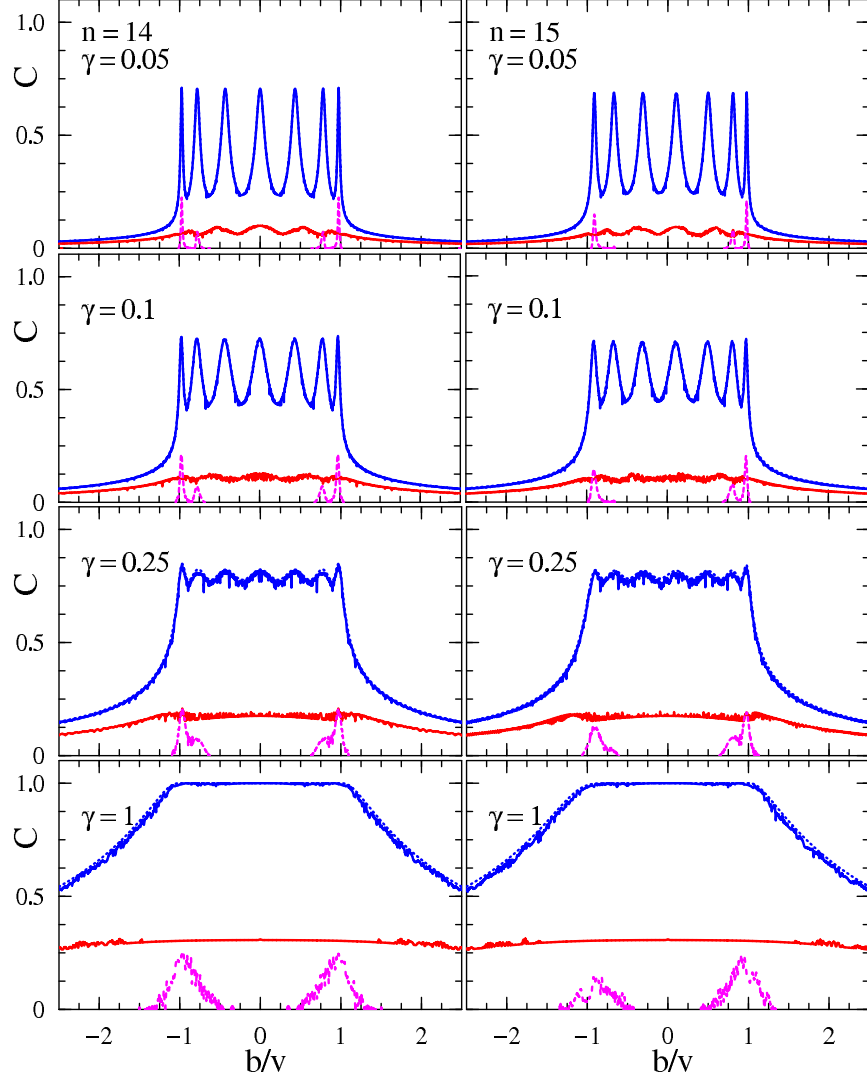


FIG. 3: (Color online) Maximum concurrence between one qubit and the rest of the chain (upper blue lines) and between adjacent qubits (lower red+dashed pink lines) in a $n = 14$ (left) and $n = 15$ (right) qubit chain for different anisotropies, reached in an interval $0 \leq vt \leq 180$. The dashed pink lines depict the maximum of the type II pairwise concurrence, which becomes now lower than the type I plateau for $\gamma \gtrsim 0.25$. Results for C_1 obtained with the upper bound (23) are also depicted (dotted lines, almost overlapping with the blue solid lines). The peaks in C_1 are visible for $\gamma \lesssim 0.4$, and saturation ($C_1 = 1$) is reached for $\gamma \gtrsim 0.92$.

in $p(t)$, we obtain, for $n \geq 5$,

$$\begin{aligned}
 p(t) &\approx \frac{1}{2}g^2t^2\left[1 - \frac{1}{12}t^2(v^2 + 4b^2 + 3g^2)\right], \\
 C_1(t) &\approx \sqrt{2}gt\left[1 - \frac{1}{24}t^2(v^2 + 4b^2 + 9g^2)/24\right].
 \end{aligned}$$

It is thus seen that for $g \gg (b, g)$ and $n \gtrsim 8$, $p(t)$ exhibits an initial peak at $t \approx 1.92/g$, where $p(t) \approx 0.7$, with $p(t) \geq 1/2$ for $1.2 \lesssim gt \lesssim 2.75$, so that in this limit saturation in C_1 is rapidly reached (see Fig. 5). The initial peak in C_1 can be correctly predicted by its 7th order expansion.

2. Evaluation of $C_2(t)$

Let us now examine the pairwise concurrence. The relevant elements (11) of the adjacent pair density are

$$\begin{aligned}\beta(t) &= \langle c_j^\dagger(t)c_{j+1}(t) \rangle_0 = \frac{2}{n} \sum'_k \frac{g^2 \cos \omega_k \sin^2 \omega_k}{\lambda_k^2} \sin^2 \lambda_k t, \\ \alpha(t) &= \langle c_j^\dagger(t)c_{j+1}^\dagger(t) \rangle_0 = \frac{2}{n} \sum'_k \frac{g \sin^2 \omega_k}{\lambda_k} \quad (29)\end{aligned}$$

$$\begin{aligned}&\times \sin \lambda_k t \left[\frac{b-v \cos \omega_k}{\lambda_k} \sin \lambda_k t - i \cos \lambda_k t \right], \\ p_1(t) &= \langle c_j^\dagger(t)c_j(t)c_{j+1}^\dagger(t)c_{j+1}(t) \rangle_0 \\ &= p^2(t) - \beta^2(t) + |\alpha^2(t)|, \quad (30)\end{aligned}$$

where $j < n$ and in (30) we have applied Wick's theorem for vacuum expectation values.

The corresponding results for $n = 4, 5$ and $14, 15$ are also depicted in Figs. 2-3. It is seen that for low g , $C_2(t)$ presents sharp type II resonances only below the outer peaks of C_1 , and actually just below the rightmost peak for small odd n . In order to understand this behavior, we note that for $g \rightarrow 0$ and $b = b_k$,

$$\beta(t) \rightarrow \frac{2}{n} \cos \omega_k \sin^2 \lambda_k t, \quad |\alpha(t)| \rightarrow \frac{1}{n} |\sin \omega_k \sin 2\lambda_k t|. \quad (31)$$

These limits can also be directly read from Eq. (27), as $(2/n) \cos \omega_k$ is the average $\langle c_j^\dagger c_{j+1} \rangle = \sum_{k'} \cos \omega_{k'} \langle c_{k'}^\dagger c_{k'} \rangle / n$ in the state $|k, -k\rangle$ whereas $\alpha(t)$ is the average $\sum_{k'} \sin \omega_{k'} \langle c_{k'}^\dagger c_{-k'}^\dagger \rangle / n$ in the full state (27). The type II maxima of C_2 are then obtained for $\sin^2 \lambda_k t = 1$, leading to

$$C_2^m \rightarrow \frac{4}{n} \left[|\cos \omega_k| - \sin \omega_k \sqrt{1 - \frac{4}{n} + \frac{4}{n^2} \sin^2 \omega_k} \right], \quad (32)$$

in this limit at $b = b_k$. Eq. (32) is actually positive for

$$\sin^2 \omega_k \leq \left[1 - \frac{2}{n} + \sqrt{\left(1 - \frac{2}{n}\right)^2 + \frac{4}{n^2}} \right]^{-1} \approx \frac{1}{2} + \frac{1}{n} + O\left(\frac{1}{n^2}\right),$$

i.e., $\omega_k \lesssim \pi/4$ or $\omega_k \gtrsim 3\pi/4$ ($|b_k|/v \gtrsim 1/\sqrt{2}$) for large n , so that they arise just beneath the outer peaks of C_1 , the strongest located at the rightmost peak for n odd ($k = 1/2$) and outermost peaks for n even ($k = 1/2$ or $[n/2] - 1/2$). Thus, type II resonances in C_2 *remain also finite for $g \rightarrow 0$* but are of order n^{-1} , becoming smaller than those of C_1 for large n ($C_2^m/C_1^m \propto \sqrt{2/n}$). The scaled concurrence nC_2^m remains nevertheless finite for large n .

For $n = 3$ we *exactly* recover from (32) the previous result $C_2^m = 2/3$ for the type II peak. For $n = 4$, Eq. (32) yields $C_2^m = (2\sqrt{2} - 1)/4 \approx 0.46$, whereas for $n = 5$ it leads to a single peak at $\omega_k = \pi/5$, of height ≈ 0.41 . For $n = 14$, there are sharp type II peaks at the outer resonances, of height ≈ 0.22 , plus smaller peaks at the next resonance, of height ≈ 0.08 , which rapidly fall below the type I plateau. For $n = 15$ the visible type II peaks are asymmetric and appear at $b_k/v \approx 0.98, 0.81$ and -0.91 , with heights $\approx 0.21, 0.08$ and 0.15 .

For $g \rightarrow 0$ there are also type I maxima of C_2 at $b = b_k$, visible in the central region (Fig. 3). These maxima are broader and occur at times determined by

$$\cos(2\lambda_k t) = \frac{1 - \frac{2}{n} \sin^2 \omega_k}{\sqrt{\sin^2 \omega_k + (1 - \frac{2}{n} \sin^2 \omega_k)^2}},$$

(the first peak at $t_1 \approx \pi/(8\lambda_k)$ for $\omega_k \approx \pi/2$), where the concurrence approaches for $g \rightarrow 0$ the value

$$C_2^m \rightarrow \frac{2}{n} [\sqrt{(1 - \frac{2}{n} \sin^2 \omega_k)^2 + \sin^2 \omega_k} - (1 - \frac{2}{n} \sin^2 \omega_k)]. \quad (33)$$

Since this is an increasing function of $|\sin \omega_k|$, i.e., a decreasing function of $|b_k|$, the type I maxima fall below those of type II for low $|\sin \omega_k|$ ($|\sin \omega_k| \lesssim 0.66$ or $|b_k|/v \gtrsim 0.75$ for large n). Moreover, at the highest type I peak ($\omega_k \approx \pi/2$), $C_2^m \approx 2(\sqrt{2} - 1)/n$ for large n , which is just 21% of the highest type II peak ($C_2^m \approx 4/n$). For $n = 3$ we also recover from (33) the previous exact result $C_2^m = 1/3$ in the type I plateau, while for $n = 2$ it yields the correct maximum value $C_2^m = 1$. For $n = 4$ and 5 we obtain $C_2^m \approx 0.14$ and $C_2^m \approx 0.07, 0.2$ at the type I peaks, while for $n = 14, 15$, $C_2^m \approx 0.07, 0.06$ at the centermost type I peak for $g \rightarrow 0$.

As g increases, the lower type I resonances in C_2^m become rapidly smoothed out, merging into a broad plateau (Figs. 2,3). Moreover, while for low n the type II peaks remain visible even for large g (Fig. 2), as n increases these peaks become as well superseded by the type I plateau (Fig. 3), which is discussed below. On the other hand, for $|b| \gg v, g$, we obtain, up to first order in $g/|b|, v/|b|$, $C_2(t) \approx 2|\alpha(t)| \leq C_2^m$, with

$$C_2^m \approx \frac{4g}{n|b|} \sum'_k \sin^2 \omega_k = \frac{g}{|b|}, \quad n \geq 3,$$

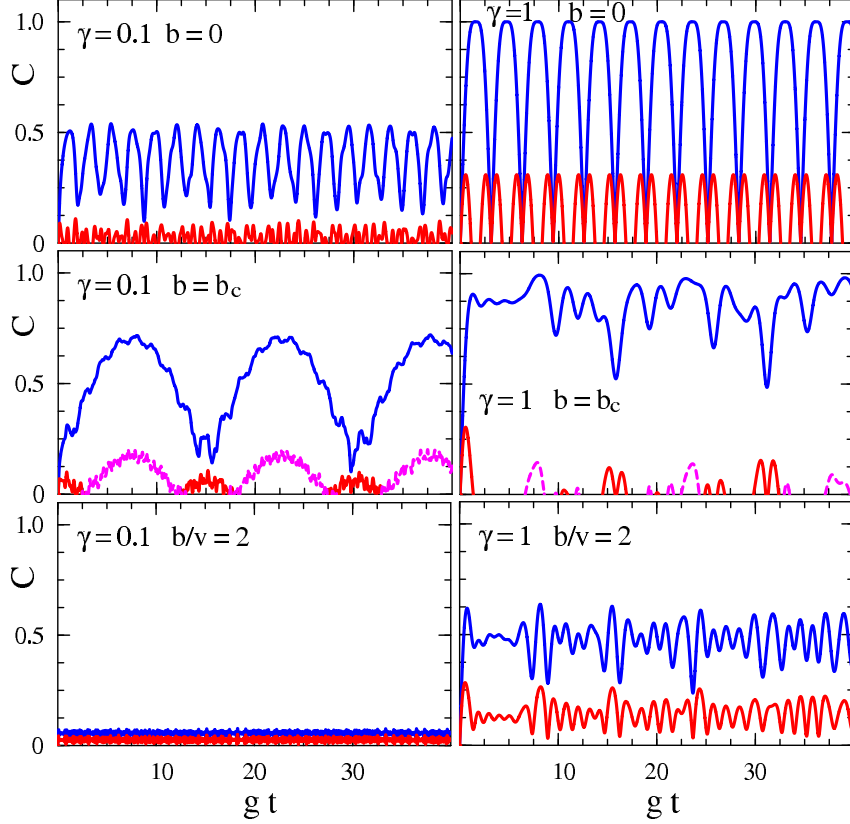


FIG. 4: (Color online). The evolution of $C_1(t)$ (upper curves in blue) and $C_2(t)$ (lower curves, in red and pink) for $n = 15$ at two different anisotropies and different fields. The central panels depict the evolution at the outer resonance $b_c/v = \cos(\pi/n) \approx 0.98$. Both the type I (red) and type II (pink, dashed lines) sectors of $C_2(t)$ are indicated.

in agreement with the previous result for $n = 3$. In this limit, $C_2^m \approx C_1^m/\sqrt{2}$.

3. Temporal Evolution

Fig. 4 depicts $C_1(t)$ and $C_2(t)$ for $n = 15$ at two different anisotropies, *at* and *away* from resonances. For low γ (left panels), we observe a low frequency periodic-like evolution of $C_1(t)$ and $C_2(t)$ at the outer resonance ($b/v \approx 0.98$), in agreement with (26) and (31), with $C_2(t)$ exhibiting regions of both type I and type II entanglement, whereas for large fields $b = 2v$ both $C_1(t)$ and $C_2(t)$ become very small, with $C_2(t)$ of type I. Both $C_1(t)$ and $C_2(t)$ are also smaller for $b = 0$ (with $C_2(t)$ again of type I), which here corresponds approximately to a minimum of C_1^m and C_2^m .

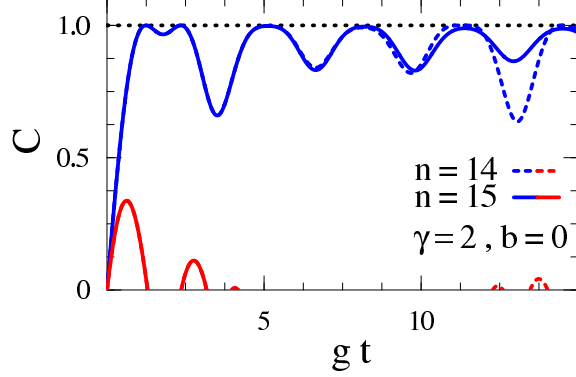


FIG. 5: (Color online). Evolution for large anisotropy and short times of $C_1(t)$ (upper curves in blue) and $C_2(t)$ (lower curves, in red), for neighboring odd-even systems.

On the other hand, for $\gamma = 1$ the emerging global entanglement is non-negligible for all moderate fields, with saturation in C_1 reached for $b \lesssim v$. In this case $C_2(t)$ does not follow the behavior of $C_1(t)$ for low fields, where it strictly vanishes at finite time intervals, although for large $b > v$ the evolution of $C_2(t)$ becomes again similar to that of $C_1(t)$ (with $C_2^m \approx C_1^m/\sqrt{2}$), and intervals of vanishing value are *removed*. Thus, the *average* pairwise entanglement is in this case *enhanced* by a large field $b \approx 2v$, in comparison with that for $b \approx v$, as a consequence of the lower global entanglement. In other words, the decoherence of the pair for large γ due to the interaction with the spin chain (representing here the environment for the pair) is prevented by large fields.

It is also seen that the evolution for $\gamma = 1$ ($g = v$) and $b = 0$ is strictly periodic. In this case $\lambda_k = v \forall k$ and Eqs. (29) become *independent* of n for $n \geq 4$ and of the form

$$p(t) = \frac{1}{2} \sin^2 vt, \quad \beta(t) = 0, \quad \alpha(t) = -i \frac{1}{4} \sin 2vt,$$

$$C_1(t) = |\sin vt| \sqrt{2 - \sin^2 vt}, \quad (34)$$

$$C_2(t) = |\sin vt| \text{Max} [|\cos vt| - |\sin vt|/2, 0]. \quad (35)$$

Hence, $C_1(t)$ reaches saturation when $|\sin vt| = 1$, whereas $C_2(t)$ has maxima when $\cos 2vt = 1/\sqrt{5}$, where $C_2(t) = (\sqrt{5} - 1)/4 \approx 0.31$, and vanishes in the interval where $|\cos vt| < 1/\sqrt{5}$ or when $\sin vt = 0$. The previous maximum of C_2 is already close to the maximum obtained for large γ (see below) and is higher than the resonant values for $n > 9$.

Fig. (5) depicts the typical evolution for short times and large anisotropy. As seen here, the plateau in the maximum concurrence C_2^m arising for $g > (v, b)$ is originated by the first maximum in the evolution of $C_2(t)$, which exhibits in this region a prominent initial “burst”

followed by intervals of vanishing value (i.e., decoherence of the pair) and lower revivals (near the most prominent minima of $C_1(t)$). For $g \gg (b, v)$ and $n \gtrsim 5$, the initial peak of C_2 occurs at $gt \approx 0.66$, with height $C_2^m \approx 0.35$, and is practically *independent* of n . The resonances in C_2^m , of order n^{-1} , become then rapidly covered by the plateau as n or g increases. This initial peak can be approximately reproduced by a fourth order expansion of $C_2(t)$, given for $n \geq 5$ by

$$C_2(t) \approx gt[1 - \frac{1}{2}gt - \frac{1}{6}t^2(v^2 + b^2 + 3g^2) + \frac{1}{12}gt^3(2b^2 + 3g^2 - v^2)].$$

Nonetheless, odd-even differences and n -dependence do arise for longer times ($gt \gtrsim 10$ in the case of Fig. 5) and affect the revivals of C_2 .

Let us finally mention that as the resonances arising for low γ develop their first maximum at $t_k = \pi/(2g \sin \omega_k)$, the relevant timescale for their observation is $\tau \approx \hbar/(\gamma v) \approx \tau_v/\gamma$, where $\tau_v \approx \hbar/v$ is the operation time associated with the hopping strength v , and should be smaller than the characteristic decoherence time τ_d of the chain determined by its interaction with the environment. This limits the smallness of the anisotropy (i.e., $\gamma \gtrsim \tau_v/\tau_d$) and hence the sharpness of the peaks. For instance, if $\gamma = 0.1$ and $v \approx 0.02$ meV, which is a typical strength for realizations based on quantum dots electron spins coupled through a cavity mode [17], $\tau \approx 3 \times 10^{-10}$ s, which is smaller than the typical decoherence time [17]. On the other hand, the results for C_2 represent the evolution of the entanglement of an adjacent pair in the present spin chain environment, and indicate that resonances remain finite at the pairwise level in such scenario.

IV. CONCLUSIONS

We have examined the entangling capabilities of a finite anisotropic XY chain with constant parameters for an initially completely aligned state in the transverse direction. The exact analytical results obtained (valid for all n) show that the maximum attainable entanglement exhibits for low anisotropy γ a clear resonant behavior as a function of the transverse magnetic field, with peaks at those fields where the effective quasiparticle energies λ_k are minimum and vanish for $\gamma = 0$. At these fields, the energy levels become then degenerate for $\gamma \rightarrow 0$ and the aligned state remains mixed with its degenerate partner for

arbitrarily small but non-zero γ . The height of these resonances remains thus finite for $\gamma \rightarrow 0$ and their width is proportional to the anisotropy, implying a fine field sensitivity apt for efficient control, although the time required to reach the peak is proportional to γ^{-1} and the height decreases as the number of qubits increases. The resonances are notorious in the maximum global entanglement between one-qubit and the rest of the chain, and are present as well in the entanglement of other global partitions.

They also arise in the maximum pairwise concurrence, and can be of both spin parities, although they are of lower height and decrease more rapidly with n , being hence more easily smoothed out for increasing γ . Here we have shown that type II (I) resonances become dominant at large (low) critical fields for adjacent pairs, those of type II being extremely narrow. Another feature is that odd-even differences in the resonant behavior remain appreciable for moderate n , odd chains exhibiting field sign sensitivity both in the global and pairwise peaks. On the other hand, saturation can be reached in the global E_1 entanglement within a certain field window above a threshold anisotropy ($\gamma \approx 1$ for large n), but not in the pairwise entanglement, whose maximum exhibits instead a broad low plateau for large γ and hence low field sensitivity. Let us finally remark that resonances of the present type will also occur for non-adjacent pairs as well as for other geometries or interaction ranges, although details (i.e., relative widths and strengths) may certainly differ from the present ones and are currently under investigation.

RR acknowledges support of CIC of Argentina.

-
- [1] E. Schrödinger, *Naturwissenschaften* **23**, 807 (1935); *Proc. Cam. Philos. Soc.* **31**, 555 (1935).
 - [2] C.H. Bennett et al., *Phys. Rev. Lett.* **70**, 1895 (1993); *Phys. Rev. Lett.* **76**, 722 (1996).
 - [3] A.K. Ekert, *Phys. Rev. Lett.* **67**, 661 (1991); *Nature* **358**, 14 (1992).
 - [4] D.P. DiVincenzo, *Science* **270**, 255 (1995).
 - [5] C.H. Bennett and D.P. DiVincenzo, *Nature (London)* **404**, 247 (2000).
 - [6] M.A. Nielsen and I. Chuang, *Quantum Computation and Quantum Information*, Cambridge Univ. Press (2000).
 - [7] C.H. Bennett, D.P. DiVincenzo, J.A. Smolin, W.K. Wootters, *Phys. Rev. A* **54**, 3824 (1996).
 - [8] S. Hill and W.K. Wootters, *Phys. Rev. Lett.* **78**, 5022 (1997); W.K. Wootters, *Phys. Rev. Lett.*

- 80**, 2245 (1998).
- [9] T.J. Osborne and M.A. Nielsen, Phys. Rev. **A 66**, 032110 (2002).
 - [10] A. Osterloh et al, Nature (London) 416, 608 (2002).
 - [11] G. Vidal, J.I. Latorre, E. Rico, A. Kitaev, Phys. Rev. Lett. **90**, 227902 (2003).
 - [12] F. Verstraete, M.A. Martin-Delgado, J.I. Cirac, Phys. Rev. Lett. **92**, 087201 (2004).
 - [13] T. Roscilde, P. Verrucchi, A. Fubini, S. Haas, V. Tognetti, Phys. Rev. Lett. **93**, 167203 (2004).
 - [14] E. Lieb, T. Schultz and D. Mattis, Ann. Phys. (NY) 16, 407 (1961).
 - [15] A. Sachdev, *Quantum Phase Transitions*, Cambridge Univ. Press (1999).
 - [16] D. Loss and D.P. DiVincenzo, Phys. Rev. **A 57**, 120 (1998); G. Burkard, D. Loss, and D.P. DiVincenzo, Phys. Rev. **B 59**, 2070 (1999).
 - [17] A. Imamoglu, D.D. Awschalom, G. Burkard, D.P. DiVincenzo, D. Loss, M. Sherwin, and A. Small, Phys. Rev. Lett. **83**, 4204 (1999).
 - [18] S.C. Benjamin, S. Bose, Phys. Rev. Lett. **90** 247901 (2003); Phys. Rev. **A 70**, 032314 (2004).
 - [19] J. Levy, Phys. Rev. Lett. **89**, 147902 (2002).
 - [20] U. Dorner, P. Fedichev, D. Jaksch, M. Lewenstein, P. Zoller, Phys. Rev. Lett. **91**, 073601 (2003); J.J. García-Ripoll, M.A. Martin-Delgado, J.I. Cirac, *ibid* **93**, 250405 (2004).
 - [21] Y. Makhlin, G. Schön and A. Shnirman, Rev. Mod. Phys. **73**, 357 (2001)
 - [22] M.C. Arnesen, S. Bose and V. Vedral, Phys. Rev. Lett. **87**, 017901 (2001).
 - [23] X. Wang, Phys. Rev. **A 66**, 044305 (2002); Phys. Rev. **A 66**, 034302 (2002).
 - [24] R. Rossignoli, N. Canosa, Phys. Rev. **A 72**, 012335 (2005); N. Canosa, R. Rossignoli, **A 73** 022347 (2006).
 - [25] L. Amico, A. Osterloh, F. Plastina, R. Fazio, G.M. Palma, Phys. Rev. **A 69** 022304 (2004).
 - [26] A. Sen(De), U. Sen, M. Lewenstein, **A 70**, 060304R (2004); *ibid* **A 72**, 052319 (2005).
 - [27] S.D.Hamieh, M.I.Katsnelson, Phys. Rev. **A 72** 032316 (2005).
 - [28] Z.Huang, S. Kais, Phys. Rev. **A 73**, 022339 (2006).
 - [29] M. Koniorczyk, P. Rapcan, V. Buzek, Phys. Rev. **A 72**, 022321 (2005).
 - [30] V. Coffman, J.Kundu, W.K. Wootters, Phys. Rev. **A 61**, 052306 (2000).
 - [31] T.J. Osborne, F. Verstraete, Phys. Rev. Lett. **96**, 220503 (2006).
 - [32] W. Dür and J.I. Cirac, Phys. Rev. **A 61**, 042314 (2000).
 - [33] P. Ring, P. Schuck, *The Nuclear Many-Body Problem*, Springer, NY (1980).